Global Knockdown of Glutamate Decarboxylase 67 Elicits Emotional and Auditory Abnormalities in Mice

Shigeo Miyata (s_miyata@gunma-u.ac.jp)
Gunma University Graduate School of Medicine School of Medicine: Gunma Daigaku Daigakuin Igakukei Kenkyuka Igakubu https://orcid.org/0000-0003-1713-805X

Toshikazu Kakizaki
Gunma University: Gunma Daigaku

Kazuyuki Fujihara
Gunma University: Gunma Daigaku

Hideru Obinata
Gunma University: Gunma Daigaku

Touko Hirano
Gunma University: Gunma Daigaku

Junichi Nakai
Tohoku University Graduate School of Dentistry School of Dentistry: Tohoku Daigaku Daigakuin Shigaku Kenkyuka Shigakubu

Mika Tanaka
RIKEN BSI: RIKEN Noshinkei Kagaku Kenkyu Center

Shigeyoshi Itohara
RIKEN BSI: RIKEN Noshinkei Kagaku Kenkyu Center

Masahiko Watanabe
Hokkaido University Graduate School of Medicine School of Medicine: Hokkaido Daigaku Daigakuin Igakuin

Kenji F Tanaka
Keio University School of Medicine Graduate School of Medicine: Keio Gijuku Daigaku Igakubu Daigakuin Igaku Kenkyuka

Manabu Abe
Niigata University: Niigata Daigaku

Kenji Sakimura
Niigata University: Niigata Daigaku

Yuchio Yanagawa
Gunma University Graduate School of Medicine School of Medicine: Gunma Daigaku Daigakuin Igakukei Kenkyuka Igakubu

Research

Keywords: Animal model, Auditory function, Behavior, GABA, Glutamate decarboxylase, Knockdown mice, Tetracycline-controlled gene expression

Posted Date: September 21st, 2020

DOI: https://doi.org/10.21203/rs.3.rs-78751/v1

Version of Record: A version of this preprint was published on January 7th, 2021. See the published version at https://doi.org/10.1186/s13041-020-00713-2.

Global knockdown of glutamate decarboxylase 67 elicits emotional and auditory abnormalities in mice

Shigeo Miyata [1]*, Toshikazu Kakizaki [1], Kazuyuki Fujihara [1], Hideru Obinata [2], Touko Hirano [2], Junichi Nakai [3], Mika Tanaka [4], Shigeyoshi Itohara [4], Masahiko Watanabe [5], Kenji F. Tanaka [6], Manabu Abe [7], Kenji Sakimura [7], Yuchio Yanagawa [1]*

[1] Department of Genetic and Behavioral Neuroscience, Gunma University Graduate School of Medicine, Gunma 371-8511, Japan

[2] Laboratory for Analytical Instruments, Education and Research Support Center, Gunma University Graduate School of Medicine, Gunma 371-8511, Japan

[3] Division of Oral Physiology, Department of Oral Function and Morphology, Tohoku University Graduate School of Dentistry, Miyagi 980-8575, Japan

[4] Laboratory for Behavioral Genetics, RIKEN Brain Science Institute, Saitama 351-0198, Japan

[5] Department of Anatomy, Hokkaido University Graduate School of Medicine, Hokkaido 060‐8638, Japan

[6] Department of Neuropsychiatry, Keio University School of Medicine, Tokyo 160-8582, Japan

[7] Department of Animal Model Development, Brain Research Institute, Niigata University, Niigata 951-8585, Japan

*Corresponding authors:

Shigeo Miyata (s_miyata@gunma-u.ac.jp) and Yuchio Yanagawa (yuchio@gunma-u.ac.jp)

Keywords: Animal model, Auditory function, Behavior, GABA, Glutamate decarboxylase, Knockdown mice, Tetracycline-controlled gene expression

Abstract

Reduced expression of glutamate decarboxylase 67 (GAD67), encoded by the *Gad1* gene, is a consistent finding in postmortem brains of patients with several psychiatric disorders, including schizophrenia, bipolar disorder and major depressive disorder. The dysfunction of GAD67 in the brain is implicated in the pathophysiology of these psychiatric disorders; however, the neurobiological consequences of GAD67 dysfunction in mature brains are not fully understood because the homozygous *Gad1* knockout is lethal in newborn mice. We hypothesized that the tetracycline-controlled gene expression/suppression system could be applied to develop global GAD67 knockdown mice that would survive into adulthood. In addition, GAD67 knockdown mice would provide new insights into the neurobiological impact of GAD67 dysfunction. Here, we developed *Gad1*$^{tTA/STOP\text{-}tetO}$ biallelic knock-in mice using *Gad1*$^{STOP\text{-}tetO}$ and *Gad1*^{tTA} knock-in mice, and compared them with *Gad1*$^{+/+}$ mice. The expression level of GAD67 protein in brains of *Gad1*$^{tTA/STOP\text{-}tetO}$ mice treated with doxycycline (Dox) was decreased by approximately 90%. The GABA content was also decreased in the brains of Dox-treated *Gad1*$^{tTA/STOP\text{-}tetO}$ mice. In the open-field test, Dox-treated *Gad1*$^{tTA/STOP\text{-}tetO}$ mice exhibited hyper-locomotor activity and decreased duration spent in the center region. In addition, acoustic startle responses were impaired in Dox-treated *Gad1*$^{tTA/STOP\text{-}tetO}$ mice. These results suggest that global reduction in GAD67 elicits emotional and auditory abnormalities in mice. These GAD67 knockdown mice will be useful for elucidating the neurobiological mechanisms of emotional abnormalities, such as anxiety symptoms associated with psychiatric disorders.

Introduction

γ-Aminobutyric acid (GABA), a major inhibitory neurotransmitter, regulates a variety of biological functions. GABA is synthesized from glutamate by glutamate decarboxylase (GAD) existing two isoforms with different molecular weights, 67 kDa (GAD67) and 65 kDa (GAD65), which are independently encoded by the *Gad1* and *Gad2* genes, respectively [1,2]. Since GAD67 and GAD65 proteins have different subcellular distributions and a cofactor association [3–6], the physiological roles of GAD67 and GAD65 may be different in the brain.

Decreased expression of the full-length *GAD1* transcript and GAD67 protein is one of the most consistent findings in the brains of subjects with several psychiatric disorders, including schizophrenia, bipolar disorder and major depressive disorder [7–12]. Alternative splicing of *GAD1* and the epigenetic state may play roles in brain development and the risk of schizophrenia [12]. Recent studies with whole exome sequencing of schizophrenic patients identified missense mutation mapping at the *GAD1* gene, which caused a reduction in GAD67 enzymatic activity by ~30% due to impaired homodimerization [13,14]. Therefore, the functional impairment of GAD67 associated with genetic mutations is involved in the neurobiological mechanisms of several psychiatric disorders. To elucidate the physiological roles of GAD67 in mature brains, a study using transgenic animals with reduced GAD67 expression would be helpful. Because homozygous *Gad1* knockout ($Gad1^{-/-}$) is lethal in newborn mice [15], conditional $Gad1^{-/-}$ mice generated with a Cre-loxP strategy have often been used for neurobiological studies [16–20]. These studies have provided much information about the function of GAD67 in targeted cells. However,

behavioral and neurochemical consequences of the global dysfunction of GAD67 in mature brains are not fully understood. Several studies have been performed to investigate GAD67 function using mice with GAD67 haplodeficiency; however, physiological changes, such as GABA reduction in the brain and behavioral abnormalities, were mild in those mice [15,21–24].

The tetracycline-controlled gene expression/suppression system allows reduction in a gene of interest by administration of antibiotic tetracyclines and its derivative doxycycline (Dox) [25]. This system requires two distinct transgenic mice: one has a cell type-specific promoter driving a tetracycline-controlled transcriptional activator (tTA)-expressing allele, and the other has a tetracycline operator site (tetO) binding to tTA and driving the expression of the gene of interest. By crossing them, a biallelic knock-in mouse (tTA/tetO) can be obtained with a tTA-mediated gene induction system, which can be turned off by the administration of Dox.

We hypothesized that the tetracycline-controlled gene expression/suppression system could be applied to generate transgenic mice able to postnatally knockdown GAD67. In brief, two knock-in mice were generated: (1) *Gad1*$^{\text{STOP-tetO}}$ knock-in mice, which were generated by inserting the tetO sequence following the STOP sequence upstream of the *Gad1* translation initiation site (Fig. 1a), and (2) *Gad1*$^{\text{tTA}}$ knock-in mice [26], which express tTA proteins under the control of an endogenous *Gad1* promoter (Fig. 1b). The *Gad1*$^{\text{tTA/STOP-tetO}}$ mice can produce GAD67 protein (Fig. 1c) and survive into adulthood. In addition, the expression of GAD67 protein in the *Gad1*$^{\text{tTA/STOP-tetO}}$ mice is suppressed by treatment with Dox (Fig. 1d). Therefore, Dox-treated *Gad1*$^{\text{tTA/STOP-tetO}}$ mice

84 can be used as GAD67 knockdown mice for studying the behavioral and neurochemical consequences of the
85 global loss of GAD67 in mature brains. In this study, we successfully developed *Gad1*$^{STOP\text{-}tetO}$ knock-in mice and
86 the subsequent *Gad1*$^{tTA/STOP\text{-}tetO}$ mice. Herein, we report the behavioral abnormalities elicited by the global
87 knockdown of GAD67 in mice.

88

89 ## Methods

90 ### *Ethics*

91 This study was performed in accordance with the Guidelines for Animal Experimentation at Gunma
92 University Graduate School of Medicine and was approved by the Gunma University Ethics Committee (Permit
93 number: 14-006 and 19-009). Every effort was made to minimize the number of animals used and their suffering.

94

95 ### *Experimental design*

96 We first generated *Gad1*$^{STOP\text{-}tetO}$ knock-in mice and assessed the *Gad1* knockout phenotypes (GAD67
97 deletion, neonatal death and cleft palate) of homozygous *Gad1*$^{STOP\text{-}tetO/STOP\text{-}tetO}$ mice to confirm the elimination of
98 *Gad1* gene function by inserting the Neo-STOP-tetO cassette. We then crossed heterozygous *Gad1*$^{tTA/+}$ and
99 *Gad1*$^{STOP\text{-}tetO/+}$ mice to obtain *Gad1*$^{tTA/STOP\text{-}tetO}$ mice and confirmed tTA-mediated GAD67 expression. Afterward,
100 we evaluated whether tTA-mediated GAD67 expression was suppressed by treatment with Dox. It has been

reported that GAD67 haplodeficient mice demonstrate an approximately 40% reduction in GAD67 protein in the brain compared with wild-type mice [27]. Therefore, we judged that GAD67 knockdown mice were successfully developed when the expression level of GAD67 protein in the brain was reduced by more than 40%. These experiments were performed in mice of both sexes.

In the behavioral tests, male mice were only used. We prepared two independent cohorts comparing *Gad1*$^{+/+}$ mice and *Gad1*$^{tTA/STOP\text{-}tetO}$ mice at the ages of 8 to 10 weeks. One cohort was used for assessing the body weights, motor coordination performance, and GABA and glutamate contents in their brains. The body weights and motor coordination performance of the mice were measured 3 weeks after starting Dox treatment. Immediately after the motor coordination test, the mice were killed by decapitation, and the frontal cortex (FCX), hippocampus (HIP) and cerebellum (CER) were quickly dissected. The collected tissues were immediately frozen in liquid nitrogen and stored at -80°C until use. The frozen tissues were used for measuring GABA and glutamate contents. Another cohort was used for the open-field test and PPI test. Three weeks after treatment with Dox, the open-field test was conducted. After testing, the mice were returned to their home cage, and treatment with Dox was continued. Two days after the open-field test, the acoustic startle responses and prepulse inhibition (PPI) responses were assessed in the mice.

Animals

To generate *Gad1*$^{\text{STOP-tetO}}$ knock-in mice, we constructed the *Gad1* targeting vector by linking the following elements in tandem: the 4.7-kb 5′-homology arm, 3.4-kb Neo-STOP-tetO cassette [28], 5.9-kb 3′-homology arm, and the MC1 promoter-driven diphtheria toxin A subunit gene (DT) (Fig. 1a). The Neo-STOP-tetO cassette comprised the 1.7-kb PGK-Neo cassette, a 1.3-kb STOP sequence, and a 0.5-kb tetO site. The targeting vector was designed to insert the Neo-STOP-tetO cassette just upstream of the *Gad1* translation initiation site. We used B6-derived embryonic cells for homologous recombination. From 179 G418-resistant clones, we obtained 46 recombinant clones. Germline-transmitted offspring were established as *Gad1*$^{\text{STOP-tetO}}$ knock-in mice (Fig. 1a).

The generation of *Gad1*$^{\text{tTA}}$ knock-in mice has already been described [26]. In these mice, the *tTA2* cDNA followed by the SV40 polyadenylation signal was inserted into exon 1 of the *Gad1* gene in frame with the translation initiation codon, and the tTA protein was expressed under the control of an endogenous *Gad1* promoter (Fig. 1b).

Heterozygous mice carrying one STOP-tetO allele (*Gad1*$^{\text{STOP-tetO/+}}$ mice) were crossed with heterozygous mice carrying one tTA allele (*Gad1*$^{\text{tTA/+}}$ mice) to obtain four genotypes: *Gad1*$^{+/+}$, *Gad1*$^{\text{tTA/+}}$, *Gad1*$^{\text{STOP-tetO/+}}$ and *Gad1*$^{\text{tTA/STOP-tetO}}$ mice. To prevent the expression of GAD67 protein, we administered 100 mg of Dox per kg of regular mouse chow CE-2 (CLEA Japan, Inc.).

The animals were housed at 2-3 mice per cage (16.5 × 27 × 12.5 (H) cm) and had free access to food and water. The animal rooms for breeding and experiments were maintained at 22 ± 3°C with a 12-h light-dark cycle

(lights on at 6:00, lights off at 18:00).

Genotyping

Genotyping of the transgenic mice was performed by PCR using tail genomic DNA with SapphireAmp Fast PCR master mix (Takara Bio Inc., Japan) and the specific primer sets. Primer set 1 determined the existence of the *Neo* allele (Fig. 1a); the sequences were Neo-F, 5'- CAGCTGTGCTCGACGTTGTC-3' and Neo-R, 5'-AAGACCGGCTTCCATCCGAG-3'. Primer set 2 determined the existence of the *Gad1* and *tTA*-inserted *Gad1* alleles (Fig. 1b); the sequences were Gad1-F, 5'- TGGTCTCCCTTCTGTCTCCGA-3', Gad1-R, 5'-TGTAGGGCGCAGGTTGGTAG-3', and tTA-R, 5'-GGGCAAAAGTGAGTATGGTGCC-3'. After amplification, 5 μL of each reaction mixture and a size marker (Loading Quick 100 bp DNA Ladder, TOYOBO Co. Ltd, Osaka, Japan) were analyzed by 2% agarose gel electrophoresis, and the bands were then visualized by ethidium bromide staining. The lengths of the amplified DNA fragments were 224 bp (*Neo* allele), 229 bp (*Gad1* allele) and 357 bp (*tTA*-inserted *Gad1* allele) (Figs. 1e and 1f).

Palate formation

Mouse neonates were killed by decapitation, and the lower jaw was removed. The cleft palate of the mouse was determined under a stereoscopic microscope.

152

153 ***Immunoblot analysis***

154 The mice were killed by decapitation. The brain hemispheres of neonates and the FCX, HIP and CER of
155 adult mice were quickly dissected on an ice-cold stainless plate. The tissues were immediately frozen in liquid
156 nitrogen and stored at -80°C until use. The frozen tissues were homogenized in ice-cold buffered sucrose (0.32 M)
157 solution containing 20 mM Tris-HCl (pH 7.5) and protease inhibitor cocktail (P8340, Sigma-Aldrich, Inc.). The
158 homogenates were centrifuged at 1,000 g for 10 min at 4°C, and the supernatants were collected as the protein
159 samples. The protein concentrations were determined using a TaKaRa BCA Protein Assay Kit (T9300A, Takara
160 Bio Inc., Japan).

161 The protein samples were diluted with electrophoresis sample buffer. Proteins (1.5 μg) were separated by 8%
162 SDS-polyacrylamide gels and transferred to a PVDF membrane. Blots were probed with respective antibodies to
163 GAD65/67 (1:1,000, rabbit polyclonal antibody) [29] and GAD67 (1:1,000, mouse monoclonal antibody,
164 Millipore, Code No. MAB5406). Immunoblots were developed using horseradish peroxidase-conjugated
165 secondary antibodies (GE Healthcare) and then detected with chemiluminescence reagents (ECL prime, GE
166 Healthcare) and visualized by the Light Capture AE-9672 (ATTO Co., Ltd.). After the detection of immunoblots,
167 the blotting membranes were washed with PBS several times and reprobed with a mouse monoclonal antibody to
168 β-actin (1:10,000, Medical & Biological Laboratories Co. Ltd., Code No. M177-3). The immunoblots of β-actin

were developed and visualized by the same protocol described above. The density of the bands was determined using ImageJ software. The band densities of β-actin were used as the loading control. The relative expression level of GAD67 to β-actin was calculated and used for comparisons between the genotypes.

Double-label immunofluorescence analysis

Deeply anesthetized mice by continuous inhalation of isoflurane were fixed by perfusion with Mildform 10N (containing 3.7 - 4.3 w/w% formaldehyde; FUJIFILM Wako Pure Chemical Co., Osaka, Japan) through the left ventricle. The brain was removed and postfixed in Mildform 10N overnight at 4°C. The brain hemispheres were cut into 50-μm-thick sagittal sections by a vibrating blade tissue slicer (Neo-LinearSlicer MT, Dosaka EM Co.,Ltd., Kyoto, Japan).

Free-floating immunostaining was performed by using a VECTOR M.O.M.® (Mouse on Mouse) Immunodetection Kit (BMK-2202, Vector Laboratories Inc., USA). The sections were incubated overnight at room temperature in the 1st primary antibodies against GAD67 (1:300, mouse monoclonal antibody, MAB5406, Millipore) and parvalbumin (PV) (1:300, guinea pig polyclonal antibody, PV-GP-Af1000, Frontier Institute Co. Ltd., Hokkaido, Japan) with the M.O.M. Blocking reagent after preincubation with 0.3% Triton X-100 in PBS. After rinsing, the sections were incubated in the M.O.M. Biothinylated Anti-Mouse IgG Reagent (1:300) with a secondary antibody (1:300, goat anti-guinea pig IgG conjugated with AlexaFluor488, A-11073, Invitrogen) for 30

186 min at room temperature. After rinsing, the sections were incubated in a solution containing
187 Streptavidin-DyLight649 (1:50, SA-5649, Vector Lab.) and DAPI (1:500, D523, Dojindo Laboratories, Japan) for
188 30 min at room temperature. The stained sections were mounted on MAS-coated glass slides (Matsunami Glass
189 Ind., Ltd., Osaka, Japan) with Fluoromount (K024, Diagnostic BioSystems, USA). Fluorescence images were
190 captured with a fluorescence digital microscope (BZ-X800, Keyence, Osaka, Japan).

191 Three independent mice in the respective groups were assessed. The names of brain regions were referenced
192 to the Allen Mouse Brain Atlas (https://alleninstitute.org/).

193

194 ***Motor coordination test***

195 The performance of motor coordination in mice was tested by a rotarod apparatus (Ugo Basile, Comerio,
196 Italy) according to a previous report [16]. Briefly, each mouse was placed in a separate lane of the apparatus on a
197 rotating cylinder (3 cm diameter) at 20 rounds per minute. The latency until the mouse fell from the cylinder (up
198 to 120 s) was recorded in three consecutive trials with 2 - 3 min intervals, and the median latency was used for the
199 following analysis. If the mouse did not fall within 120 s, the latency to fall was recorded as 120 s.

200

201 ***Open-field test***

202 Each mouse was placed in the center of an open-field apparatus (50 cm × 50 cm × 40 (H) cm) that was

illuminated by light-emitting diodes (30 lux at the center of the field) and allowed to move freely for 5 min. The data were collected and analyzed using ImageJ OF4 (O'Hara & Co., Ltd., Tokyo, Japan), which is modified software that is also based on the public domain ImageJ program. The procedure was performed according to our previous report [30].

Acoustic startle response and PPI test

An acoustic startle reflex measurement system (O'Hara & Co., Ltd., Tokyo, Japan) was used. The startle response was assessed with various stimulus intensities. Five times of 70 to 120 dB (70, 75, 80, 85, 90, 95, 100, 110, and 120 dB) white noise stimuli (40 ms) were presented in quasi-random order and random intertrial intervals (10 - 20 s). In the PPI session, mice experienced five trial types: no stimulus; startle stimulus (120 dB, 40 ms) only; prepulse 70 dB (20 ms, lead time 100 ms) and pulse 120 dB; prepulse 75 dB (20 ms, lead time 100 ms) and pulse 120 dB; and prepulse 80 dB (20 ms, lead time 100 ms) and pulse 120 dB. Each trial was repeated 10 times in quasi-random order and random intertrial intervals (10 - 20 s). PPI was defined as the percent decline of the startle response: 100 - [(startle amplitude after prepulse and pulse)/(startle amplitude after pulse only)] × 100. The procedure was performed according to our previous report [19].

GABA and glutamate contents in the brains

220 The frozen tissues were weighed and then homogenized by BioMasher II (Nippi, Inc., Tokyo, Japan) in 500
221 μL of 0.1% formic acid in acetonitrile (Wako, Tokyo, Japan) containing an internal standard
222 2-morpholinoethanesulfonic acid (2-MES; Dojindo, Tokyo, Japan). The standard was spiked at a final
223 concentration of 10 μM. The homogenates were centrifuged at 15,000 g for 15 min at 4°C, and then, the
224 supernatants were collected and filtered through an ISOLUTE PLD+ column (Biotage Japan Ltd., Tokyo, Japan).
225 The 40 μL filtrates were lyophilized and stored at -20°C.

226 At the time of analysis, the lyophilized samples were dissolved in 1.25 mL of ultrapure water. The prepared
227 sample solutions (3 μL) were then injected on ultra-performance liquid chromatograph coupled to
228 triple-quadrupole mass spectrometer (LC/MS) (LCMS-8050; Shimadzu, Kyoto, Japan). The chromatographic
229 conditions were according to the Shimadzu method package using a pentafluorophenylpropyl (PFPP) column. The
230 MS settings, data acquisition and data analysis were in accordance with the manufacturer's instructions for
231 analyzing Primary Metabolites version 2.0 (Cat. #: 225-24865A, Shimadzu). The relative values of metabolites
232 from the internal standard 2-MES and the weight of corresponding tissues were calculated and used for the
233 following data analysis.

234 Standard solutions containing GABA (A2129, Sigma-Aldrich Co. LLC., USA) and L-glutamic acid (G1251,
235 Sigma-Aldrich) at dose ranges of 0.01 - 3 μmol/L and 0.03 - 10 μmol/L, respectively, with internal standard
236 2-MES (10 μM) were also applied to the LC/MS system. The concentrations of GABA and glutamate in the

sample solutions were determined by the peak heights of the chromatogram. The GABA and glutamate contents per the corresponding tissue weights were calculated.

Statistical analysis

Statistical analyses were conducted using BellCurve for Excel ver. 3.20 (Social Survey Research Information Co., Ltd., Tokyo, Japan). Significant differences among the multiple groups were analyzed by the Bonferroni multiple comparison test after one-way analysis of variance (ANOVA). Significant differences between two groups were analyzed by Student's *t*-test. The factorial comparisons in some experiments were performed by two-way ANOVA. Data are expressed as the mean with standard error (SE). Statistical significance was defined as a p value less than 0.05.

Results

Generation of Gad1$^{STOP\text{-}tetO}$ knock-in mice

To confirm the elimination of function of the *Gad1* gene by inserting the Neo-STOP-tetO cassette, we first generated homozygous *Gad1*$^{\text{STOP-tetO/STOP-tetO}}$ mice by crossing heterozygous *Gad1*$^{\text{STOP-tetO/+}}$ parents and assessed whether the *Gad1*$^{\text{STOP-tetO/STOP-tetO}}$ mouse showed the *Gad1* knockout phenotypes. *Gad1*$^{\text{STOP-tetO/STOP-tetO}}$ mice, *Gad1*$^{\text{STOP-tetO/+}}$ mice and *Gad1*$^{+/+}$ mice were born at the expected Mendelian frequency (Fig. 2a). Then, mouse

pups were divided into two groups to determine the survival rates and palate formation. All *Gad1*$^{STOP\text{-}tetO/STOP\text{-}tetO}$ mice died within 1 day after birth, but *Gad1*$^{STOP\text{-}tetO/+}$ mice and *Gad1*$^{+/+}$ mice survived (Fig. 2b). All *Gad1*$^{STOP\text{-}tetO/+}$ and *Gad1*$^{+/+}$ mice formed normal palate. However, 57% of *Gad1*$^{STOP\text{-}tetO/STOP\text{-}tetO}$ mice exhibited a cleft palate (Fig. 2c). These phenotypes are the same as those of *Gad1*$^{-/-}$ mice previously reported [31]. Western blot analyses demonstrated that the expression of GAD67 protein in the brain was abolished in *Gad1*$^{STOP\text{-}tetO/STOP\text{-}tetO}$ mice with or without cleft palate (Figs. 2d and 2e). These observations indicate that the insertion of the Neo-STOP-tetO cassette following the *Gad1* promoter eliminates the function of the *Gad1* gene in mice.

Development of GAD67 knockdown mice

We then crossed heterozygous male *Gad1*$^{tTA/+}$ mice and female *Gad1*$^{STOP\text{-}tetO/+}$ mice to generate *Gad1*$^{tTA/STOP\text{-}tetO}$ biallelic knock-in mice. Mice with four genotypes (*Gad1*$^{+/+}$, *Gad1*$^{tTA/+}$, *Gad1*$^{STOP\text{-}tetO/+}$, *Gad1*$^{tTA/STOP\text{-}tetO}$) were born at the expected Mendelian frequency (Fig. 3 *legend*). Palate formation in mouse neonates with four genotypes was observed, but none of them exhibited the cleft palate (Fig. 3a). Next, the survival rates of these mice were examined in a small population. All *Gad1*$^{+/+}$ mice (total n = 15) survived until 8 weeks of age (Fig. 3b). Two *Gad1*$^{tTA/+}$ mice (total n = 15), one *Gad1*$^{STOP\text{-}tetO/+}$ mouse (total n = 17), and eight *Gad1*$^{tTA/STOP\text{-}tetO}$ mice (total n = 20) died within 8 weeks after birth (Fig. 3b). The proportion of genotypes in our breeding colony (total n = 1,319) at the weaning period (P21 - P28) is shown in Fig. 3c. These observations

271 indicate that the survival rate of *Gad1*$^{tTA/STOP\text{-}tetO}$ mice was lower than that of mice with the other genotypes. The
272 protein levels of GAD67 in the FCX ($F(3,8) = 4.355$, $p = 0.043$, one-way ANOVA) and HIP ($F(3,8) = 10.527$, $p =$
273 0.004, one-way ANOVA) were significantly lower in *Gad1*$^{tTA/STOP\text{-}tetO}$ mice than *Gad1*$^{+/+}$ mice at 8 weeks of age
274 (Figs. 3d and 3e). On the other hand, the protein levels of GAD67 in the CER were not significantly different
275 among the genotypes ($F(3,8) = 2.867$, $p = 0.104$, one-way ANOVA) (Fig. 3f).

276 Next, the expression levels of GAD67 protein in the brains of *Gad1*$^{tTA/STOP\text{-}tetO}$ mice were examined in the
277 absence and presence of Dox treatment. We noticed that some *Gad1*$^{tTA/STOP\text{-}tetO}$ mice died during the 3 weeks after
278 starting the Dox treatment. Approximately 44% of *Gad1*$^{tTA/STOP\text{-}tetO}$ mice survived just after 3 weeks of Dox
279 treatment (Fig. 4a). The expression levels of GAD67 protein in the FCX ($F(3,8) = 20.563$, $p < 0.001$, one-way
280 ANOVA), HIP ($F(3,8) = 189.298$, $p < 0.001$, one-way ANOVA) and CER ($F(3,8) = 22.760$, $p < 0.001$, one-way
281 ANOVA) were significantly decreased by treatment with Dox in *Gad1*$^{tTA/STOP\text{-}tetO}$ mice compared with *Gad1*$^{+/+}$
282 mice (Figs. 4b – 4d). Importantly, the expression level of GAD67 protein in the CER of *Gad1*$^{tTA/STOP\text{-}tetO}$ mice was
283 markedly decreased in the presence of Dox compared with in the absence of Dox (Fig. 4d). By
284 immunofluorescence, GAD67 immunoreactivity in *Gad1*$^{+/+}$ mice was detected widely in the brain, particulary at
285 high levels in the olfactory bulb, globus pallidum, olfactory tubercle, substantia nigra, superior and inferior
286 colliculi, and deep cerebellar nuclei (Fig. 4e, upper panel). In brains of *Gad1*$^{tTA/STOP\text{-}tetO}$ mice, the overall
287 immunoreactivity was reduced moderately without Dox treatment and severely with the treatment. Dox treatment
288 to *Gad1*$^{+/+}$ mice did not affect GAD67 immunoreactivity (data not shown). PV is expressed in a major subclass of

289 GAD67-positive inhibitory neurons [32]. No discernible changes in PV immunoreactivity were found between
290 *Gad1*$^{+/+}$ mice and *Gad1*$^{tTA/STOP\text{-}tetO}$ mice with or without Dox treatment (Fig. 4e, lower panel). We assessed 3
291 independent mice in the respective groups and observed similar findings. These results suggest that Dox treatment
292 globally suppresses the expression of GAD67 in the brains of *Gad1*$^{tTA/STOP\text{-}tetO}$ mice.

293

294 ***Behavioral abnormalities in GAD67 knockdown mice***

295 We compared the behavioral phenotypes of *Gad1*$^{tTA/STOP\text{-}tetO}$ mice with those of *Gad1*$^{+/+}$ mice in the presence
296 of Dox treatment. To avoid the effects of sex differences, male mice were only used in the following experiments.

297 We first investigated the body weights and the performance of motor coordination in Dox-treated
298 *Gad1*$^{tTA/STOP\text{-}tetO}$ and *Gad1*$^{+/+}$ mice. No difference was observed in the body weights ($t(17) = 1.066$, $p = 0.301$,
299 Student's *t*-test, Fig. 5a) or the latency to fall from the cylinder in the rotarod test ($t(17) = 0.772$, $p = 0.451$,
300 Student's *t*-test, Fig. 5b) between the two genotypes.

301 We next conducted the open-field test, which is a well-accepted behavioral test to evaluate the anxiety-like
302 state of rodents [33]. The total distance, total duration of movement, moving speed, distance per movement, and
303 duration per movement were significantly increased in Dox-treated *Gad1*$^{tTA/STOP\text{-}tetO}$ mice compared with
304 Dox-treated *Gad1*$^{+/+}$ mice (Table 1). In contrast, the total number of movement episodes was significantly
305 decreased in Dox-treated *Gad1*$^{tTA/STOP\text{-}tetO}$ mice compared with Dox-treated *Gad1*$^{+/+}$ mice (Table 1). These

observations indicate that *Gad1*$^{tTA/STOP\text{-}tetO}$ mice walk longer distances with less frequency. In addition, Dox-treated *Gad1*$^{tTA/STOP\text{-}tetO}$ mice walked a long time in the wall side and a short time in the center region compared with Dox-treated *Gad1*$^{+/+}$ mice (Table 1 and Fig. 5c), indicating that *Gad1*$^{tTA/STOP\text{-}tetO}$ mice exhibited anxiety-like behavior in the open-field test.

We further assessed acoustic startle responses and PPI responses in Dox-treated *Gad1*$^{tTA/STOP\text{-}tetO}$ and *Gad1*$^{+/+}$ mice. The PPI response provides an operational index of sensorimotor gating, and an impaired PPI response is observed in subjects with schizophrenia [34]. The amplitude of acoustic startle responses was significantly affected by the effect of genotype × sound level interaction ($F(8,168) = 2.745$, $p = 0.007$, two-way ANOVA). The simple main effect of genotypes was statistically significant at the sound levels of 110 dB ($F(1, 92) = 6.345$, $p = 0.014$) and 120 dB ($F(1, 92) = 13.550$, $p < 0.001$) (Fig. 5d). The PPI responses were significantly affected by the effect of prepulse intensity ($F(2,42) = 6.713$, $p = 0.003$, two-way ANOVA) but not by the effect of genotype × prepulse intensity interaction ($F(2,42) = 0.577$, $p = 0.566$, two-way ANOVA) or genotype ($F(1,21) = 0.514$, $p = 0.481$, two-way ANOVA) (Fig. 5e).

Brain GABA and glutamate content in GAD67 knockdown mice

The GABA content was significantly lower in Dox-treated *Gad1*$^{tTA/STOP\text{-}tetO}$ mice than in *Gad1*$^{+/+}$ mice in the FCX, HIP and CER (Table 2). On the other hand, the glutamate content in the respective brain regions was

comparable between these genotypes (Table 2).

Discussion

We first generated *Gad1*$^{\text{STOP-tetO}}$ knock-in mice. All homozygous *Gad1*$^{\text{STOP-tetO/STOP-tetO}}$ mice died on the day of birth, and 57% of *Gad1*$^{\text{STOP-tetO/STOP-tetO}}$ mice exhibited a cleft palate. The expression of GAD67 protein was lacking in the brains of *Gad1*$^{\text{STOP-tetO/STOP-tetO}}$ mice with or without the cleft palate. These phenotypes in *Gad1*$^{\text{STOP-tetO/STOP-tetO}}$ mice are consistent with those in *Gad1*$^{-/-}$ mice [15,31]. Therefore, the function of the *Gad1* gene was eliminated by the insertion of the Neo-STOP-tetO cassette in the 5'-untranslated region of the *Gad1* gene in mice. It has been reported that neonatal death in *Gad1*$^{-/-}$ mice is caused by respiratory failure rather than impairment of suckling [15,35]. Therefore, neonatal death in *Gad1*$^{\text{STOP-tetO/STOP-tetO}}$ mice may also be caused by respiratory failure.

We next developed *Gad1*$^{\text{tTA/STOP-tetO}}$ biallelic knock-in mice by crossing *Gad1*$^{\text{tTA/+}}$ and *Gad1*$^{\text{STOP-tetO/+}}$ parents. Approximately 40% of *Gad1*$^{\text{tTA/STOP-tetO}}$ mice died on the day of birth, and the number of *Gad1*$^{\text{tTA/STOP-tetO}}$ mice at P21-P28 in our breeding colony was smaller than the numbers of mice with the other genotypes. None of the *Gad1*$^{\text{tTA/STOP-tetO}}$ mice demonstrated a cleft palate. Unexpectedly, some adult *Gad1*$^{\text{tTA/STOP-tetO}}$ mice died by treatment with Dox. Therefore, GAD67 is important for survival not only in the neonatal period but also in adulthood. However, the cause of death in Dox-treated *Gad1*$^{\text{tTA/STOP-tetO}}$ mice is currently unknown. To resolve this

question, pathological examination is required in a future study.

Adult mice with *Gad1* haplodeficiency demonstrated an approximately 40% reduction in GAD67 protein levels in the whole brain compared with *Gad1*$^{+/+}$ mice [27]. Consistently, we observed that heterozygous *Gad1*$^{tTA/+}$ and heterozygous *Gad1*$^{STOP\text{-}tetO/+}$ knock-in mice exhibited a 30 - 50% reduction in GAD67 protein levels in the FCX, HIP and CER compared with *Gad1*$^{+/+}$ mice. In the absence of Dox treatment, the expression level of GAD67 protein in *Gad1*$^{tTA/STOP\text{-}tetO}$ mice relative to *Gad1*$^{+/+}$ mice was dependent on the brain regions. In the immunoblotting analysis, the expression of GAD67 protein in the CER was comparable between *Gad1*$^{tTA/STOP\text{-}tetO}$ mice and *Gad1*$^{+/+}$ mice. However, the expression of GAD67 protein in the FCX and HIP was significantly lower in *Gad1*$^{tTA/STOP\text{-}tetO}$ mice than *Gad1*$^{+/+}$ mice. Importantly, in the presence of Dox treatment, GAD67 expression was reduced by approximately 90% in the brains of *Gad1*$^{tTA/STOP\text{-}tetO}$ mice, compared with Dox-treated *Gad1*$^{+/+}$ mice. The brain-wide reduction of GAD67 expression in Dox-treated *Gad1*$^{tTA/STOP\text{-}tetO}$ mice was also observed in the immunofluorescence analysis. These findings suggest that GAD67 expression is suppressed by treatment with Dox in the brains of *Gad1*$^{tTA/STOP\text{-}tetO}$ mice.

In adult mice with *Gad1* haplodeficiency, the GABA content in the brain was reduced by 7 - 20% from those in wild-type control mice [15,32]. In this study, we found that the GABA contents in the FCX, HIP and CER of Dox-treated *Gad1*$^{tTA/STOP\text{-}tetO}$ mice were reduced by 27.0% - 56.8% from those in Dox-treated *Gad1*$^{+/+}$ mice. Therefore, the GABA reduction in the brains of Dox-treated *Gad1*$^{tTA/STOP\text{-}tetO}$ mice was larger than that in *Gad1*

haplodeficient mice. Because approximately half of the brain GABA is produced by GAD65 in adulthood [36], the remaining GABA in the brain of Dox-treated *Gad1*$^{tTA/STOP\text{-}tetO}$ mice is mainly synthesized by GAD65. The brain glutamate contents in Dox-treated *Gad1*$^{tTA/STOP\text{-}tetO}$ mice were comparable to those in Dox-treated *Gad1*$^{+/+}$ mice. Therefore, the glutamatergic system may be normal in Dox-treated *Gad1*$^{tTA/STOP\text{-}tetO}$ mice.

GAD67 haplodeficient mice demonstrated several abnormal behaviors, such as hyper-locomotor activity, reduced interactions with an unfamiliar mouse, and aggressive behavior. However, the emotional behaviors in *Gad1* haplodeficient mice were normal in the open-field test, the light-dark avoidance test and the elevated plus-maze test [21,23]. In the current open-field test, Dox-treated *Gad1*$^{tTA/STOP\text{-}tetO}$ mice walked longer distances than Dox-treated *Gad1*$^{+/+}$ mice. In addition, Dox-treated *Gad1*$^{tTA/STOP\text{-}tetO}$ mice preferentially walked for more time along the walls and for less time in the center region. These observations indicate that Dox-treated *Gad1*$^{tTA/STOP\text{-}tetO}$ mice exhibited behavioral abnormalities, including the hyper-locomotor activity and anxiety-like behavior, in the open-field test. Since *Gad1*$^{tTA/STOP\text{-}tetO}$ mice exhibited normal body weight and motor coordination in the presence of Dox treatment, the changes in exploratory behavior are unlikely to be associated with physical dysfunction. It is well accepted that inhibition of GABAergic tone elicits anxiety-like behavior in the open-field test [33]. Therefore, the reduction in brain GABA in Dox-treated *Gad1*$^{tTA/STOP\text{-}tetO}$ mice may cause the induction of anxiety-like behavior. The mice lacking GAD67 in protein phosphatase 1 regulatory subunit 2 (Ppp1r2)-expressing cells, in which Cre recombinase expression is largely confined to GABA interneurons of the cerebral cortex and the hippocampus, demonstrated the hyper-locomotor activity and anxiety-like behavior in the

375 open-field test [37]. In addition, we recently reported that mice lacking GAD67 in somatostatin-expressing GABA
376 interneurons demonstrated anxiety-like behavior in the open-field test without affecting locomotor activity [20].
377 Therefore, the anxiety-like behavior in Dox-treated *Gad1*$^{tTA/STOP\text{-}tetO}$ mice may be due to GAD67 knockdown from
378 somatostatin-expressing GABA interneurons in cortical and hippocampal areas. In addition, the hyper-locomotor
379 activity in Dox-treated *Gad1*$^{tTA/STOP\text{-}tetO}$ mice may be associated with GAD67 knockdown from the other subtypes
380 of GABA interneurons.

381 In this study, Dox-treated *Gad1*$^{tTA/STOP\text{-}tetO}$ mice showed a normal response to PPI. Therefore, global
382 knockdown of GAD67 does not affect the PPI response. However, we previously reported that mice with
383 conditional *Gad1* heterozygous knockout predominantly in parvalbumin-positive cells demonstrated an impaired
384 response to PPI [19]. It is possible that a mild reduction in GAD67 in parvalbumin-positive cells might be
385 required for impairing the PPI response. Interestingly, the startle responses elicited by large acoustic stimuli were
386 impaired in Dox-treated *Gad1*$^{tTA/STOP\text{-}tetO}$ mice. GABAergic interneurons expressing GAD67 proteins constitute
387 auditory neural networks and contribute to auditory function [38–40]. Therefore, it is possible that global
388 knockdown of GAD67 in the brain induces the impairment of auditory function.

389 The *GAD1* gene and GAD67 protein have often been targeted in human studies to elucidate an association
390 with the pathophysiology of psychiatric disorders [41–43]. Reduced full-length *GAD1* transcript and GAD67
391 protein is a consistent finding in the postmortem brains of patients with several psychiatric disorders including

schizophrenia, bipolar disorder and major depressive disorder [7–12]. Because GAD67 reduction was predominantly observed in parvalbumin-positive GABAergic interneurons in the postmortem brains of schizophrenic patients [44–46], mice with conditional knockout of GAD67 in parvalbumin-positive cells have been used as an animal model of schizophrenia [18,19,47,48]. On the other hand, the specific subsets of GABAergic interneurons reducing GAD67 expression have not yet been identified in other psychiatric disorders, which might indicate that GAD67 expression is globally reduced in the brain of subjects with the other psychiatric disorders. In this study, global knockdown of GAD67 elicited anxiety-like behavior in mice. Therefore, we suggest the possibility that the global reduction in *GAD1* transcript and GAD67 protein in the brain might be related to the occurrence of anxiety symptoms frequently comorbid in several psychiatric disorders.

We did not examine whether administration of anxiolytic, antidepressant or antipsychotic drugs improves anxiety-like behavior in Dox-treated *Gad1*$^{tTA/STOP\text{-}tetO}$ mice. Because of the high lethality rate, we could not immediately prepare a sufficient number of animals for conducting a pharmacological study. Therefore, we will determine the utility of Dox-treated *Gad1*$^{tTA/STOP\text{-}tetO}$ mice as a tool for screening potential medications for anxiety symptoms in a future study.

In summary, *Gad1*$^{tTA/STOP\text{-}tetO}$ biallelic knock-in mice showed GAD67-knockdown phenotypes when treated with Dox. We suggest that the global reduction in GAD67 elicits emotional and auditory abnormalities in mice. The use of GAD67 knockdown mice will provide new insights into the neurobiological impact of GAD67

dysfunction and elucidate the neurobiological mechanisms of emotional abnormalities associated with psychiatric disorders.

Abbreviations

GAD67: glutamate decarboxylase 67; GAD65: glutamate decarboxylase 65; Dox: doxycycline; GABA: γ-aminobutyric acid; tTA: tetracycline-controlled transcriptional activator; tetO: tetracycline operator site; FCX: frontal cortex; HIP: hippocampus; CER: cerebellum; CP: cleft palate; PV: parvalbumin; PPI: prepulse inhibition; ANOVA: analysis of variance; SE: standard error

Declarations

Ethics approval and consent to participate

This study was performed in accordance with the Guidelines for Animal Experimentation at Gunma University Graduate School of Medicine and was approved by the Gunma University Ethics Committee (Permit number: 14-006 and 19-009). Every effort was made to minimize the number of animals used and their suffering.

Consent for publication

Not applicable.

Availability of data and materials

All data are available within the manuscript.

Competing interests

The authors declare that they have no conflicts of interest with the contents of this manuscript.

Funding

This work was supported by the Japan Society for the Promotion of Science (JSPS) KAKENHI Grant Number 26290002 (YY), 15H05872 (YY), 17H05550 (YY), 19K06881 (YY) and 16H06276 (AdAMS) (KS). This work was the result of using research equipment shared in MEXT Project for promoting public utilization of advanced research infrastructure (Program for supporting introduction of the new sharing system) Grant Number JPMXS0420600120. This project was partly supported by the Takeda Science Foundation (YY).

Authors' contributions

S.M. and Y.Y. conceptualization; S.M. data curation; S.M. formal analysis; Y.Y. and K.S. funding acquisition; S.M., H.O. and T.H. investigation; S.M., T.K., K.F. and Y.Y. methodology; S.M. project administration; J.N., M.T., S.I., M.W., K.T., M.A. and K.S. resources; Y.Y. supervision; S.M. and Y.Y. writing-original draft; all authors writing-review&editing.

Acknowledgments

We are grateful to Dr. Kunihiko Obata for his encouragement. We would like to thank Yukari Shiba for her help with animal care and experiments. We also thank the staff at the Bioresource Center of Gunma University Graduate School of Medicine for technical support.

References

1. Ji F, Kanbara N, Obata K. GABA and histogenesis in fetal and neonatal mouse brain lacking both the isoforms of glutamic acid decarboxylase. Neurosci Res. 1999;33:187–94.

2. Soghomonian JJ, Martin DL. Two isoforms of glutamate decarboxylase: why? Trends Pharmacol Sci. 1998;19:500–5.

3. Esclapez M, Tillakaratne NJ, Kaufman DL, Tobin AJ, Houser CR. Comparative localization of two forms of glutamic acid decarboxylase and their mRNAs in rat brain supports the concept of functional differences between the forms. J Neurosci. Society for Neuroscience; 1994;14:1834–55.

4. Obata K, Fukuda T, Konishi S, Ji F-Y, Mitoma H, Kosaka T. Synaptic localization of the 67,000 mol. wt isoform of glutamate decarboxylase and transmitter function of GABA in the mouse cerebellum lacking the 65,000 mol. wt isoform. Neuroscience. Pergamon; 1999;93:1475–82.

5. Martin DL, Martin SB, Wu SJ, Espina N. Regulatory properties of brain glutamate decarboxylase (GAD): the apoenzyme of GAD is present principally as the smaller of two molecular forms of GAD in brain. J Neurosci. J Neurosci; 1991;11:2725–31.

6. Martin DL, Martin SB, Wu SJ, Espina N. Cofactor interactions and the regulation of glutamate decarboxylase activity. Neurochem Res. 1991;16:243–9.

7. Guidotti A, Auta J, Davis JM, Gerevini VD, Dwivedi Y, Grayson DR, et al. Decrease in Reelin and Glutamic Acid Decarboxylase67 (GAD67) Expression in Schizophrenia and Bipolar Disorder. Arch Gen Psychiatry. American Medical Association; 2000;57:1061–9.

8. Hashimoto T, Arion D, Unger T, Maldonado-Avilés JG, Morris HM, Volk DW, et al. Alterations in GABA-related transcriptome in the dorsolateral prefrontal cortex of subjects with schizophrenia. Mol Psychiatry. Nature Publishing Group; 2008;13:147–61.

9. Volk DW, Austin MC, Pierri JN, Sampson AR, Lewis DA. Decreased Glutamic Acid Decarboxylase67 Messenger RNA Expression in a Subset of Prefrontal Cortical γ-Aminobutyric Acid Neurons in Subjects With Schizophrenia. Arch Gen Psychiatry. American Medical Association; 2000;57:237.

10. Karolewicz B, Maciag D, O'Dwyer G, Stockmeier CA, Feyissa AM, Rajkowska G. Reduced level of glutamic acid decarboxylase-67 kDa in the prefrontal cortex in major depression. Int J Neuropsychopharmacol. 2010;13:411–20.

11. Scifo E, Pabba M, Kapadia F, Ma T, Lewis DA, Tseng GC, et al. Sustained Molecular Pathology Across Episodes and Remission in Major Depressive Disorder. Biol Psychiatry. 2018;83:81–9.

12. Tao R, Davis KN, Li C, Shin JH, Gao Y, Jaffe AE, et al. GAD1 alternative transcripts and DNA methylation in human prefrontal cortex and hippocampus in brain development, schizophrenia. Mol Psychiatry. Nature Publishing Group; 2018;23:1496–505.

13. Giacopuzzi E, Gennarelli M, Minelli A, Gardella R, Valsecchi P, Traversa M, et al. Exome sequencing in schizophrenic patients with high levels of homozygosity identifies novel and extremely rare mutations in the GABA/glutamatergic pathways. Al-Aama JY, editor. PLoS One. Public Library of Science; 2017;12:e0182778.

14. Magri C, Giacopuzzi E, La Via L, Bonini D, Ravasio V, Elhussiny MEA, et al. A novel homozygous mutation in GAD1 gene described in a schizophrenic patient impairs activity and dimerization of GAD67 enzyme. Sci Rep. Nature Publishing Group; 2018;8:15470.

15. Asada H, Kawamura Y, Maruyama K, Kume H, Ding RG, Kanbara N, et al. Cleft palate and decreased brain gamma-aminobutyric acid in mice lacking the 67-kDa isoform of glutamic acid decarboxylase. Proc Natl Acad Sci U S A. 1997;94:6496–9.

16. Obata K, Hirono M, Kume N, Kawaguchi Y, Itohara S, Yanagawa Y. GABA and synaptic inhibition of mouse cerebellum lacking glutamate decarboxylase 67. Biochem Biophys Res Commun. 2008;370:429–33.

17. Heusner CL, Beutler LR, Houser CR, Palmiter RD. Deletion of GAD67 in dopamine receptor-1 expressing cells causes specific motor deficits. genesis. John Wiley & Sons, Ltd; 2008;46:357–67.

18. Kuki T, Fujihara K, Miwa H, Tamamaki N, Yanagawa Y, Mushiake H. Contribution of parvalbumin and somatostatin-expressing GABAergic neurons to slow oscillations and the balance in beta-gamma oscillations across cortical layers. Front Neural Circuits. 2015;9:6.

19. Fujihara K, Miwa H, Kakizaki T, Kaneko R, Mikuni M, Tanahira C, et al. Glutamate Decarboxylase 67 Deficiency in a Subset of GABAergic Neurons Induces Schizophrenia-Related Phenotypes. Neuropsychopharmacology. Nature Publishing Group; 2015;40:2475–86.

20. Miyata S, Kumagaya R, Kakizaki T, Fujihara K, Wakamatsu K, Yanagawa Y. Loss of Glutamate Decarboxylase 67 in Somatostatin-Expressing Neurons Leads to Anxiety-Like Behavior and Alteration in the Akt/GSK3β Signaling Pathway. Front Behav Neurosci. Frontiers; 2019;13:131.

21. Sandhu K V., Lang D, Müller B, Nullmeier S, Yanagawa Y, Schwegler H, et al. Glutamic acid decarboxylase

67 haplodeficiency impairs social behavior in mice. Genes, Brain Behav. John Wiley & Sons, Ltd (10.1111); 2014;13:439–50.

22. Chen L, McKenna JT, Leonard MZ, Yanagawa Y, McCarley RW, Brown RE. GAD67-GFP knock-in mice have normal sleep-wake patterns and sleep homeostasis. Neuroreport. 2010;21:216–20.

23. Smith KM. Hyperactivity in mice lacking one allele of the glutamic acid decarboxylase 67 gene. ADHD Atten Deficit Hyperact Disord. 2018;10:267–71.

24. Nullmeier S, Elmers C, D'Hanis W, Sandhu KVK, Stork O, Yanagawa Y, et al. Glutamic acid decarboxylase 67 haplodeficiency in mice: consequences of postweaning social isolation on behavior and changes in brain neurochemical systems. Brain Struct Funct. Springer Berlin Heidelberg; 2020;225:1719–42.

25. Das AT, Tenenbaum L, Berkhout B. Tet-On Systems For Doxycycline-inducible Gene Expression. Curr Gene Ther. Bentham Science Publishers Ltd.; 2016;16:156–67.

26. Tanaka KF, Matsui K, Sasaki T, Sano H, Sugio S, Fan K, et al. Expanding the Repertoire of Optogenetically Targeted Cells with an Enhanced Gene Expression System. Cell Rep. Cell Press; 2012;2:397–406.

27. Wang Y, Kakizaki T, Sakagami H, Saito K, Ebihara S, Kato M, et al. Fluorescent labeling of both GABAergic and glycinergic neurons in vesicular GABA transporter (VGAT)-Venus transgenic mouse. Neuroscience. Neuroscience; 2009;164:1031–43.

28. Tanaka KF, Ahmari SE, Leonardo ED, Richardson-Jones JW, Budreck EC, Scheiffele P, et al. Flexible

525 Accelerated STOP Tetracycline Operator-Knockin (FAST): A Versatile and Efficient New Gene Modulating
526 System. Biol Psychiatry. Elsevier; 2010;67:770–3.

527 29. Hanamura K, Mizui T, Kakizaki T, Roppongi RT, Yamazaki H, Yanagawa Y, et al. Low accumulation of
528 drebrin at glutamatergic postsynaptic sites on GABAergic neurons. Neuroscience. 2010;169:1489–500.

529 30. Miyata S, Kurachi M, Okano Y, Sakurai N, Kobayashi A, Harada K, et al. Blood transcriptomic markers in
530 patients with late-onset major depressive disorder. PLoS One. 2016;11:e0150262.

531 31. Kakizaki T, Oriuchi N, Yanagawa Y. GAD65/GAD67 double knockout mice exhibit intermediate severity in
532 both cleft palate and omphalocele compared with GAD67 knockout and VGAT knockout mice. Neuroscience.
533 2015;288:86–93.

534 32. Tamamaki N, Yanagawa Y, Tomioka R, Miyazaki JI, Obata K, Kaneko T. Green Fluorescent Protein
535 Expression and Colocalization with Calretinin, Parvalbumin, and Somatostatin in the GAD67-GFP Knock-In
536 Mouse. J Comp Neurol. 2003;467:60–79.

537 33. Prut L, Belzung C. The open field as a paradigm to measure the effects of drugs on anxiety-like behaviors: A
538 review. Eur. J. Pharmacol. Elsevier; 2003. p. 3–33.

539 34. Braff DL, Geyer MA, Swerdlow NR. Human studies of prepulse inhibition of startle: Normal subjects, patient
540 groups, and pharmacological studies. Psychopharmacology (Berl). Psychopharmacology (Berl); 2001. p.
541 234–58.

35. Kuwana S, Okada Y, Sugawara Y, Tsunekawa N, Obata K. Disturbance of neural respiratory control in neonatal mice lacking gaba synthesizing enzyme 67-kda isoform of glutamic acid decarboxylase. Neuroscience. Pergamon; 2003;120:861–70.

36. Stork O, Ji F-Y, Kaneko K, Stork S, Yoshinobu Y, Moriya T, et al. Postnatal development of a GABA deficit and disturbance of neural functions in mice lacking GAD65. Brain Res. Elsevier; 2000;865:45–58.

37. Kolata SM, Nakao K, Jeevakumar V, Farmer-Alroth EL, Fujita Y, Bartley AF, et al. Neuropsychiatric Phenotypes Produced by GABA Reduction in Mouse Cortex and Hippocampus. Neuropsychopharmacology. Nature Publishing Group; 2018;43:1445–56.

38. Burianova J, Ouda L, Profant O, Syka J. Age-related changes in GAD levels in the central auditory system of the rat. Exp Gerontol. Exp Gerontol; 2009;44:161–9.

39. Turner JG, Parrish JL, Zuiderveld L, Darr S, Hughes LF, Caspary DM, et al. Acoustic experience alters the aged auditory system. Ear Hear. Ear Hear; 2013;34:151–9.

40. Ito T, Inoue K, Takada M. Distribution of glutamatergic, GABAergic, and glycinergic neurons in the auditory pathways of macaque monkeys. Neuroscience. Elsevier Ltd; 2015;310:128–51.

41. Cherlyn SYT, Woon PS, Liu JJ, Ong WY, Tsai GC, Sim K. Genetic association studies of glutamate, GABA and related genes in schizophrenia and bipolar disorder: A decade of advance. Neurosci. Biobehav. Rev. Neurosci Biobehav Rev; 2010. p. 958–77.

559 42. Lacerda-Pinheiro SF, Pinheiro Junior RFF, De Lima MAP, Da Silva CGL, Dos Santos MDSV, Teixeira
560 Júnior AG, et al. Are there depression and anxiety genetic markers and mutations? A systematic review. J.
561 Affect. Disord. Elsevier; 2014. p. 387–98.

562 43. Mitchell AC, Jiang Y, Peter C, Akbarian S. Transcriptional regulation of GAD1 GABA synthesis gene in the
563 prefrontal cortex of subjects with schizophrenia. Schizophr. Res. Elsevier; 2015. p. 28–34.

564 44. Hashimoto T, Volk DW, Eggan SM, Mirnics K, Pierri JN, Sun Z, et al. Gene expression deficits in a subclass
565 of GABA neurons in the prefrontal cortex of subjects with schizophrenia. J Neurosci. Society for Neuroscience;
566 2003;23:6315–26.

567 45. Curley AA, Arion D, Volk DW, Asafu-Adjei JK, Sampson AR, Fish KN, et al. Cortical deficits of glutamic
568 acid decarboxylase 67 expression in schizophrenia: Clinical, protein, and cell type-specific features. Am J
569 Psychiatry. Am J Psychiatry; 2011;168:921–9.

570 46. Kimoto S, Zaki MM, Holly Bazmi H, Lewis DA. Altered Markers of Cortical γ-aminobutyric acid neuronal
571 activity in schizophrenia role of the NARP gene. JAMA Psychiatry. American Medical Association;
572 2015;72:747–56.

573 47. Brown JA, Ramikie TS, Schmidt MJ, Báldi R, Garbett K, Everheart MG, et al. Inhibition of
574 parvalbumin-expressing interneurons results in complex behavioral changes. Mol Psychiatry. Nature
575 Publishing Group; 2015;20:1499–507.

576 48. Georgiev D, Yoshihara T, Kawabata R, Matsubara T, Tsubomoto M, Minabe Y, et al. Cortical gene
577 expression after a conditional knockout of 67 kda glutamic acid decarboxylase in parvalbumin neurons.
578 Schizophr Bull. 2016;42:992–1002.

579

580

Legends for Figures

Fig. 1. Doxycycline (Dox)-regulated *Gad1* suppression system. (a) Generation of *Gad1*$^{\text{STOP-tetO}}$ knock-in mice. Schematic diagram depicting *Gad1* genomic DNA (*Gad1*$^{+}$), targeting vector, and *Gad1* genomic DNA inserted into the Neo-STOP-tetO cassette (*Gad1*$^{\text{STOP-tetO}}$). Arrows indicate the PCR primers (Primer set 1). (b) Schematic representation of *Gad1* genomic DNA (*Gad1*$^{+}$) and DNA containing the tetracycline-controlled transactivator (tTA) gene (*Gad1*$^{\text{tTA}}$). Arrows indicate the PCR primers (Primer set 2). (c, d) Schematic diagram of the Dox-regulated *Gad1* suppression system in *Gad1*$^{\text{tTA/STOP-tetO}}$ mice. Before Dox treatment, tTA binds to the tetracycline operator site (tetO) and promotes *Gad1* transcription and GAD67 production (c). Dox treatment interferes with tTA binding to tetO and suppresses *Gad1* transcription (d). Representative results of PCR genotyping for *Gad1*$^{\text{tTA/STOP-tetO}}$ mice (e), *Gad1*$^{\text{STOP-tetO/STOP-tetO}}$ mice (f) and their littermates. M; 100-bp size marker, +/+; *Gad1*$^{+/+}$, tTA/tet; *Gad1*$^{\text{tTA/STOP-tetO}}$, tTA/+; *Gad1*$^{\text{tTA/+}}$, tet/+; *Gad1*$^{\text{STOP-tetO/+}}$, tet/tet; *Gad1*$^{\text{STOP-tetO/STOP-tetO}}$.

Fig. 2. Characterization of homozygous *Gad1*$^{\text{STOP-tetO/STOP-tetO}}$ mice. (a) The number of mouse pups born from heterozygous *Gad1*$^{\text{STOP-tetO/+}}$ parents. +/+; *Gad1*$^{+/+}$, tet/+; *Gad1*$^{\text{STOP-tetO/+}}$, tet/tet; *Gad1*$^{\text{STOP-tetO/STOP-tetO}}$. (b) The survival rates of mouse pups born from heterozygous *Gad1*$^{\text{STOP-tetO/+}}$ parents. (c) Microscopic images of the palate of mice. The arrow indicates a cleft palate (CP). (d) Representative western blot analysis of the expression of GAD65/67 and β-actin proteins in the brains of *Gad1*$^{+/+}$, *Gad1*$^{\text{STOP-tetO/+}}$ and *Gad1*$^{\text{STOP-tetO/STOP-tetO}}$ mice. (e) Western

598 blot analysis of the expression of GAD65/67 and β-actin proteins in the brains of 3 *Gad1*$^{STOP\text{-}tetO/STOP\text{-}tetO}$ mice with
599 and without CP. The *Gad1*$^{+/+}$ mouse protein sample was used as a positive control for GAD67 immunoblotting.
600
601 **Fig. 3.** Characterization of *Gad1*$^{tTA/STOP\text{-}tetO}$ mice in the absence of Dox treatment. (a) Microscopic images of the
602 palates of mice. (b) The survival rates of *Gad1*$^{+/+}$ (+/+), *Gad1*$^{tTA/STOP\text{-}tetO}$ (tTA/tet), *Gad1*$^{tTA/+}$ (tTA/+) and
603 *Gad1*$^{STOP\text{-}tetO/+}$ (tet/+) mice. The number of mice at postnatal day 0 was 15 (+/+), 20 (tTA/tet), 15 (tTA/+) and 17
604 (tet/+). (c) The number of mice with four genotypes at postnatal days 21 - 28. (d - f) Representative western blot
605 analysis of the expression of GAD65/67 and β-actin proteins in the frontal cortex (d), the hippocampus (e) and the
606 cerebellum (f) of *Gad1*$^{+/+}$, *Gad1*$^{tTA/STOP\text{-}tetO}$, *Gad1*$^{tTA/+}$ and *Gad1*$^{STOP\text{-}tetO/+}$ mice. β-Actin was used as a loading
607 control. Three independent mice of the respective genotypes were examined. The band densities of GAD67 and
608 β-actin were quantified by ImageJ software. GAD67 protein levels were normalized to β-actin protein expression,
609 and the % change was calculated relative to *Gad1*$^{+/+}$ mice. The means with SE are demonstrated as columns. *$p <$
610 0.05 vs. the value of *Gad1*$^{+/+}$ mice (Bonferroni test).
611
612 **Fig. 4.** Characterization of *Gad1*$^{tTA/STOP\text{-}tetO}$ mice in the presence of Dox treatment. (a) The survival rates of mice
613 with *Gad1*$^{+/+}$ (+/+) and *Gad1*$^{tTA/STOP\text{-}tetO}$ (tTA/tet) mice during Dox treatment (weeks 0, 1, 2, and 3). (b - d)
614 Representative western blot analysis of the expression of GAD65/67 and β-actin proteins in the frontal cortex (b),

615 the hippocampus (c) and the cerebellum (d) of *Gad1*$^{+/+}$ and *Gad1*$^{tTA/STOP\text{-}tetO}$ mice treated and not treated with Dox.
616 β-Actin was used as a loading control. Three independent mice in the respective groups were examined. The band
617 densities of GAD67 and β-actin were analyzed by ImageJ software. GAD67 protein levels were normalized to
618 β-actin protein expression, and the % change was calculated relative to *Gad1*$^{+/+}$ mice. The means with SE are
619 demonstrated as columns. *$p < 0.05$ vs. the value of nontreated *Gad1*$^{+/+}$ mice (Bonferroni test). #$p < 0.05$ vs. the
620 value of nontreated *Gad1*$^{tTA/STOP\text{-}tetO}$ mice (Bonferroni test). (e) Representative immunoreactivities of GAD67 and
621 parvalbumin (PV) proteins in the brain sections of nontreated *Gad1*$^{+/+}$ mice, nontreated *Gad1*$^{tTA/STOP\text{-}tetO}$ mice and
622 Dox-treated *Gad1*$^{tTA/STOP\text{-}tetO}$ mice. The white bars in the images indicate 2 mm length.

623

624 **Fig. 5.** Behavioral consequences of GAD67 knockdown in mice. Body weights (a) and latency to fall from a
625 cylinder in the rotarod test (b) for Dox-treated *Gad1*$^{+/+}$ and *Gad1*$^{tTA/STOP\text{-}tetO}$ mice. (c) Examples of the path
626 traveled in the open-field test by two *Gad1*$^{+/+}$ and two *Gad1*$^{tTA/STOP\text{-}tetO}$ mice treated with Dox. (d) Acoustic startle
627 responses of Dox-treated *Gad1*$^{+/+}$ and *Gad1*$^{tTA/STOP\text{-}tetO}$ mice. Startle amplitudes by the sounds indicate the startle
628 responses (A.U.). *$p < 0.05$ and ***$p < 0.001$ between genotypes (simple main effect of two-way ANOVA). (e)
629 PPI responses of Dox-treated *Gad1*$^{+/+}$ and *Gad1*$^{tTA/STOP\text{-}tetO}$ mice. PPI was defined as the percent decline in the
630 startle response (% Inhibition).

Figures

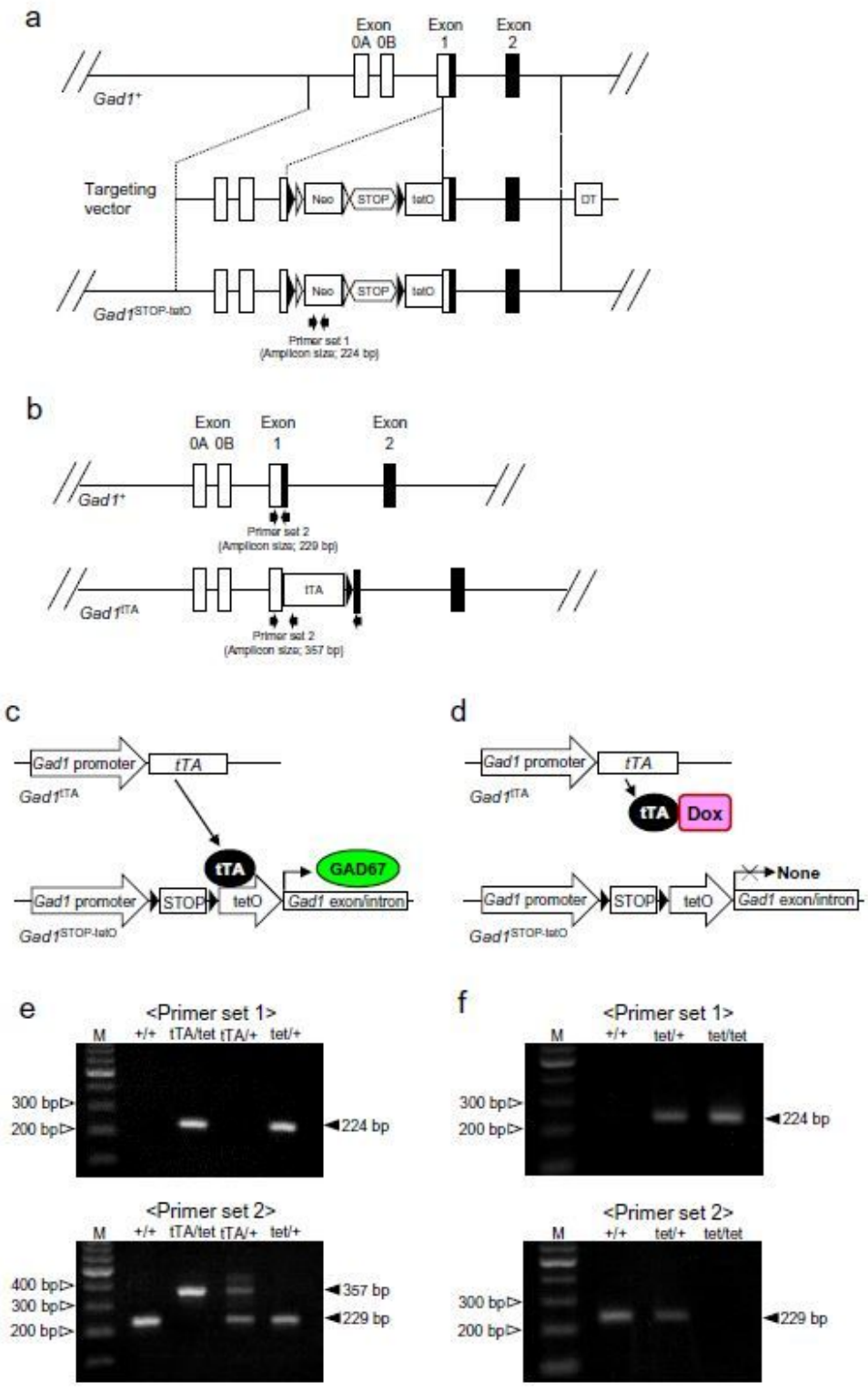

Figure 1

Doxycycline (Dox)-regulated Gad1 suppression system. (a) Generation of Gad1STOP-tetO knock-in mice. Schematic diagram depicting Gad1 genomic DNA (Gad1+), targeting vector, and Gad1 genomic DNA inserted into the Neo-STOP-tetO cassette (Gad1STOP-tetO). Arrows indicate the PCR primers (Primer set

1). (b) Schematic representation of Gad1 genomic DNA (Gad1+) and DNA containing the tetracycline-controlled transactivator (tTA) gene (Gad1tTA). Arrows indicate the PCR primers (Primer set 2). (c, d) Schematic diagram of the Dox-regulated Gad1 suppression system in Gad1tTA/STOP-tetO mice. Before Dox treatment, tTA binds to the tetracycline operator site (tetO) and promotes Gad1 transcription and GAD67 production (c). Dox treatment interferes with tTA binding to tetO and suppresses Gad1 transcription (d). Representative results of PCR genotyping for Gad1tTA/STOP-tetO mice (e), Gad1STOP-tetO/STOP-tetO mice (f) and their littermates. M; 100-bp size marker, +/+; Gad1+/+, tTA/tet; Gad1tTA/STOP-tetO, tTA/+; Gad1tTA/+, tet/+; Gad1STOP-tetO/+, tet/tet; Gad1STOP-tetO/STOP-tetO.

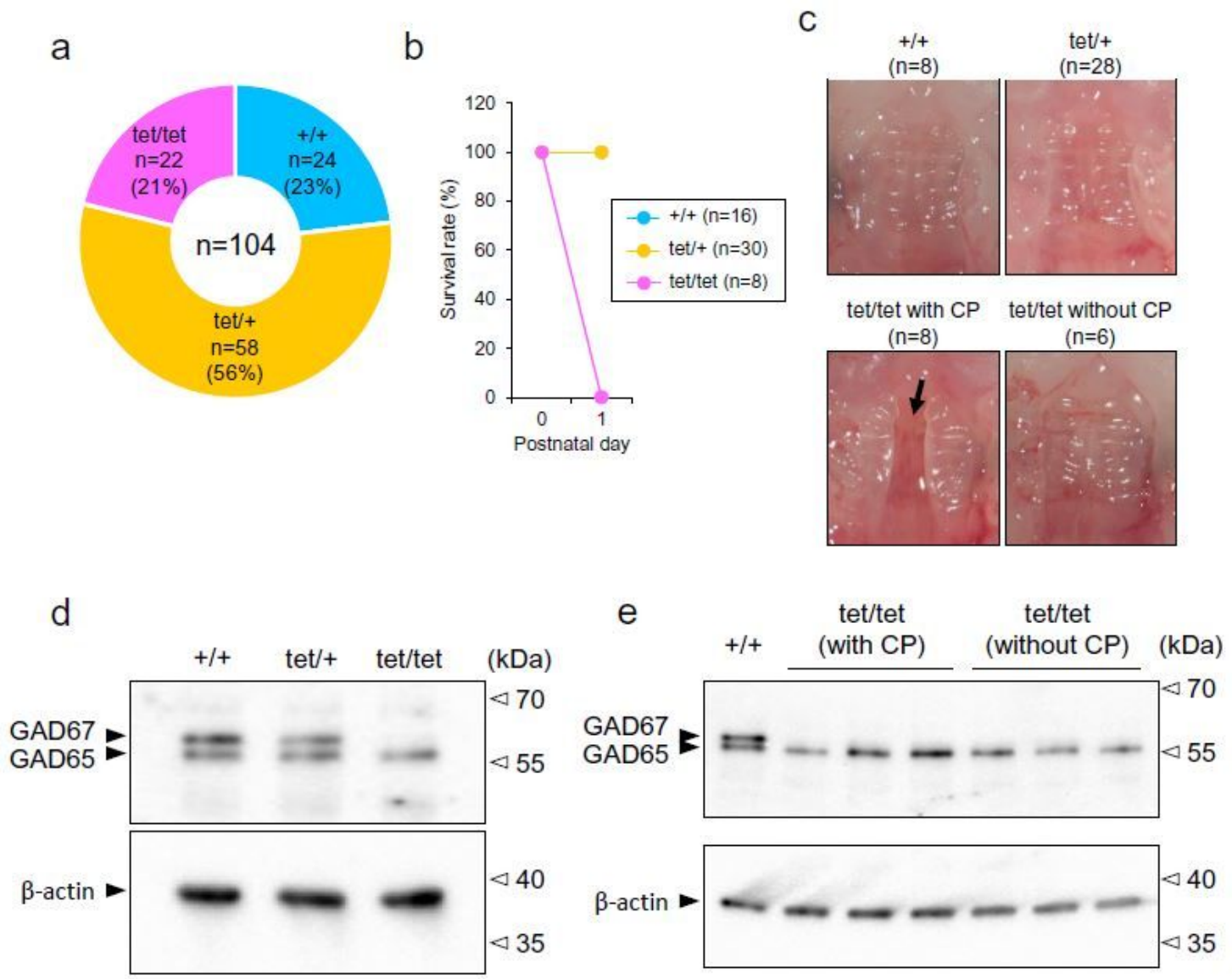

Figure 2

Characterization of homozygous Gad1STOP-tetO/STOP-tetO mice. (a) The number of mouse pups born from heterozygous Gad1STOP-tetO/+ parents. +/+; Gad1+/+, tet/+; Gad1STOP-tetO/+, tet/tet; Gad1STOP-tetO/STOP-tetO. (b) The survival rates of mouse pups born from heterozygous Gad1STOP-tetO/+ parents.

(c) Microscopic images of the palate of mice. The arrow indicates a cleft palate (CP). (d) Representative western blot analysis of the expression of GAD65/67 and β-actin proteins in the brains of Gad1+/+, Gad1STOP-tetO/+ and Gad1STOP-tetO/STOP-tetO mice. (e) Western blot analysis of the expression of GAD65/67 and β-actin proteins in the brains of 3 Gad1STOP-tetO/STOP-tetO mice with and without CP. The Gad1+/+ mouse protein sample was used as a positive control for GAD67 immunoblotting.

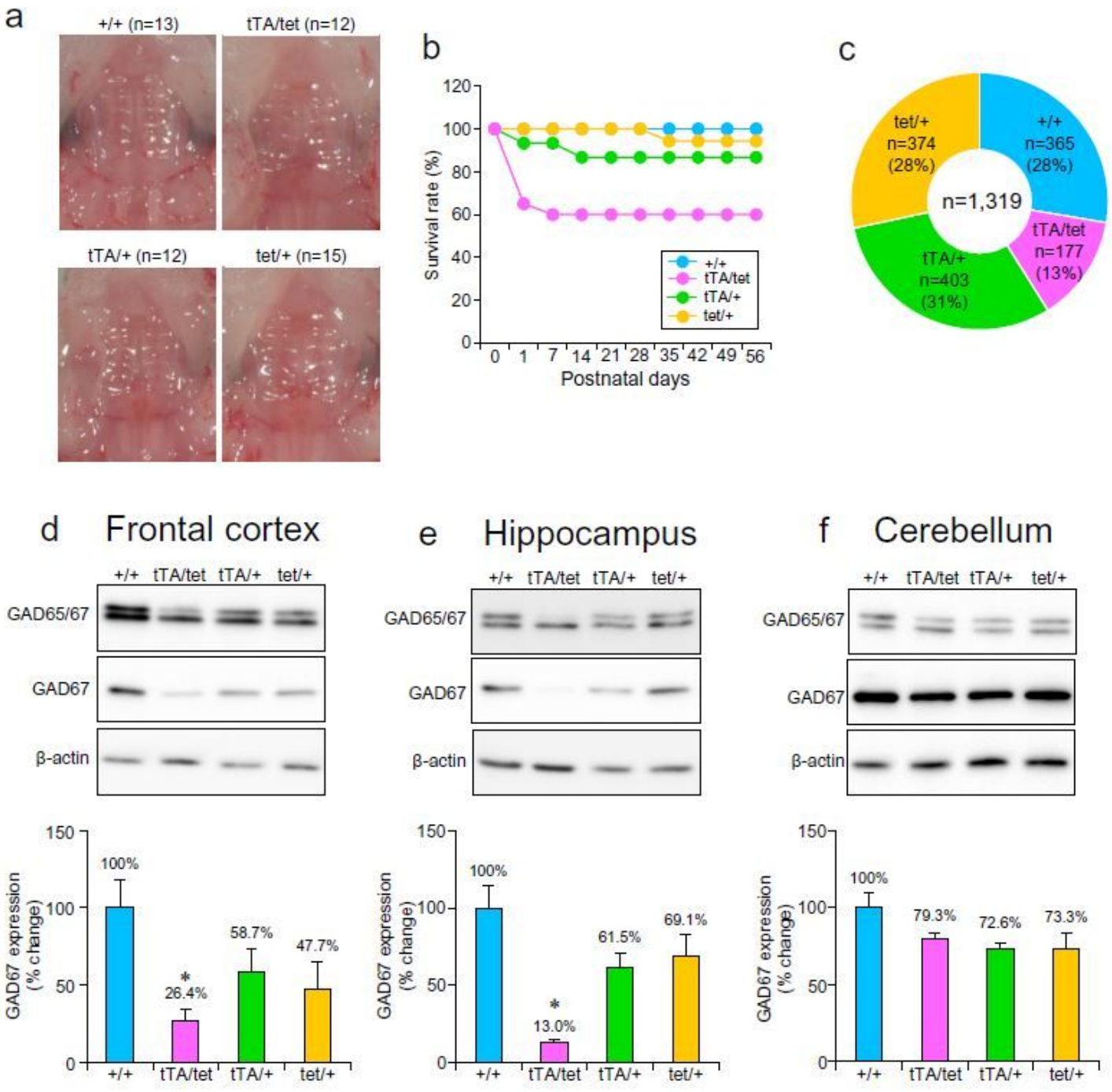

Figure 3

Characterization of Gad1tTA/STOP-tetO mice in the absence of Dox treatment. (a) Microscopic images of the palates of mice. (b) The survival rates of Gad1+/+ (+/+), Gad1tTA/STOP-tetO (tTA/tet), Gad1tTA/+

(tTA/+) and Gad1STOP-tetO/+ (tet/+) mice. The number of mice at postnatal day 0 was 15 (+/+), 20 (tTA/tet), 15 (tTA/+) and 17 (tet/+). (c) The number of mice with four genotypes at postnatal days 21 - 28. (d - f) Representative western blot analysis of the expression of GAD65/67 and β-actin proteins in the frontal cortex (d), the hippocampus (e) and the cerebellum (f) of Gad1+/+, Gad1tTA/STOP-tetO, Gad1tTA/+ and Gad1STOP-tetO/+ mice. β-Actin was used as a loading control. Three independent mice of the respective genotypes were examined. The band densities of GAD67 and β-actin were quantified by ImageJ software. GAD67 protein levels were normalized to β-actin protein expression, and the % change was calculated relative to Gad1+/+ mice. The means with SE are demonstrated as columns. *p < 0.05 vs. the value of Gad1+/+ mice (Bonferroni test).

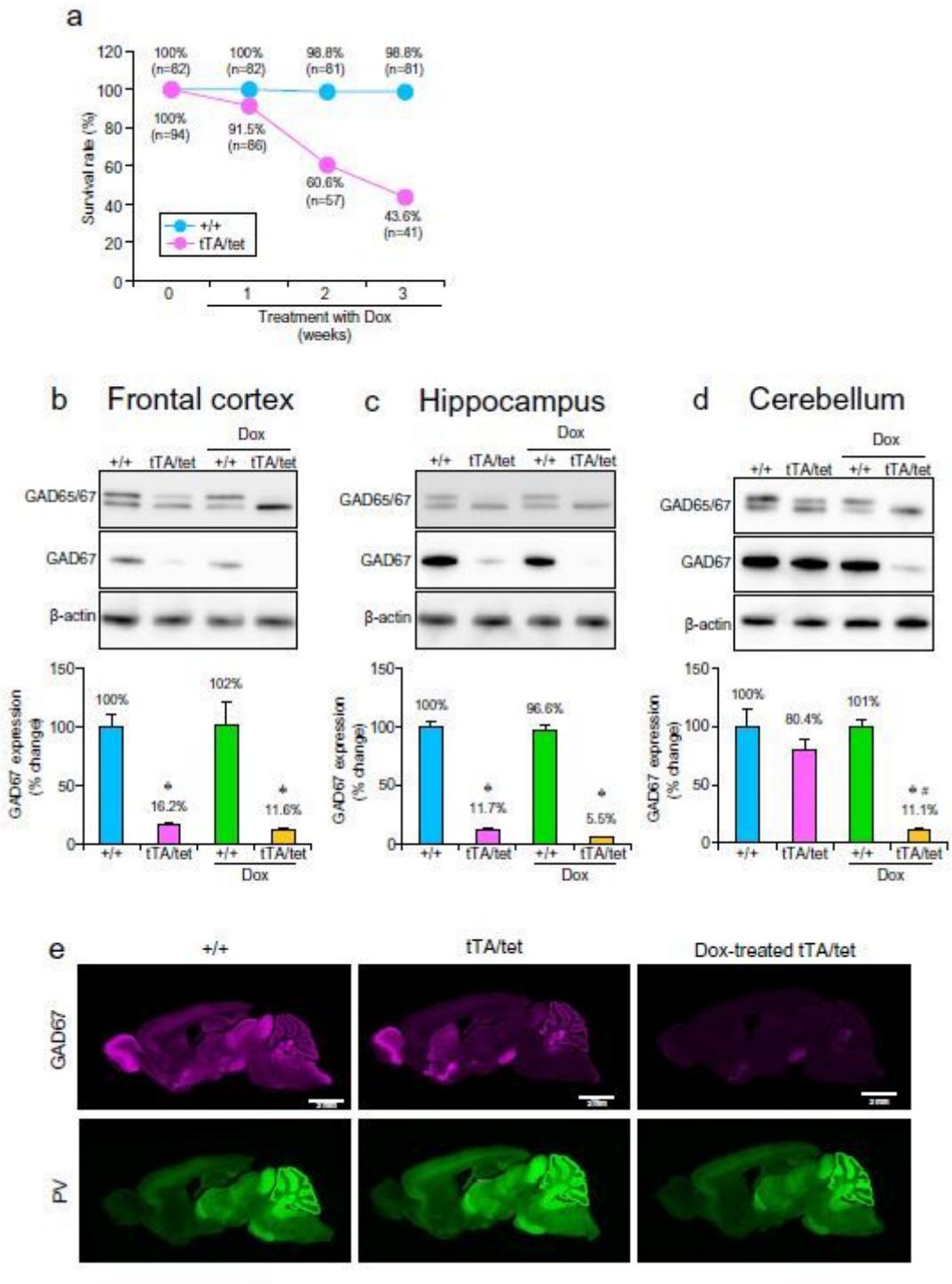

Figure 4

Characterization of Gad1tTA/STOP-tetO mice in the presence of Dox treatment. (a) The survival rates of mice with Gad1+/+ (+/+) and Gad1tTA/STOP-tetO (tTA/tet) mice during Dox treatment (weeks 0, 1, 2, and 3). (b - d) Representative western blot analysis of the expression of GAD65/67 and β-actin proteins in the frontal cortex (b), the hippocampus (c) and the cerebellum (d) of Gad1+/+ and Gad1tTA/STOP-tetO mice treated and not treated with Dox. β-Actin was used as a loading control. Three independent mice in the respective groups were examined. The band densities of GAD67 and β-actin were analyzed by ImageJ software. GAD67 protein levels were normalized to β-actin protein expression, and the % change was calculated relative to Gad1+/+ mice. The means with SE are demonstrated as columns. *$p < 0.05$ vs. the value of nontreated Gad1+/+ mice (Bonferroni test). #$p < 0.05$ vs. the value of nontreated Gad1tTA/STOP-tetO mice (Bonferroni test). (e) Representative immunoreactivities of GAD67 and parvalbumin (PV) proteins in the brain sections of nontreated Gad1+/+ mice, nontreated Gad1tTA/STOP-tetO mice and Dox-treated Gad1tTA/STOP-tetO mice. The white bars in the images indicate 2 mm length.

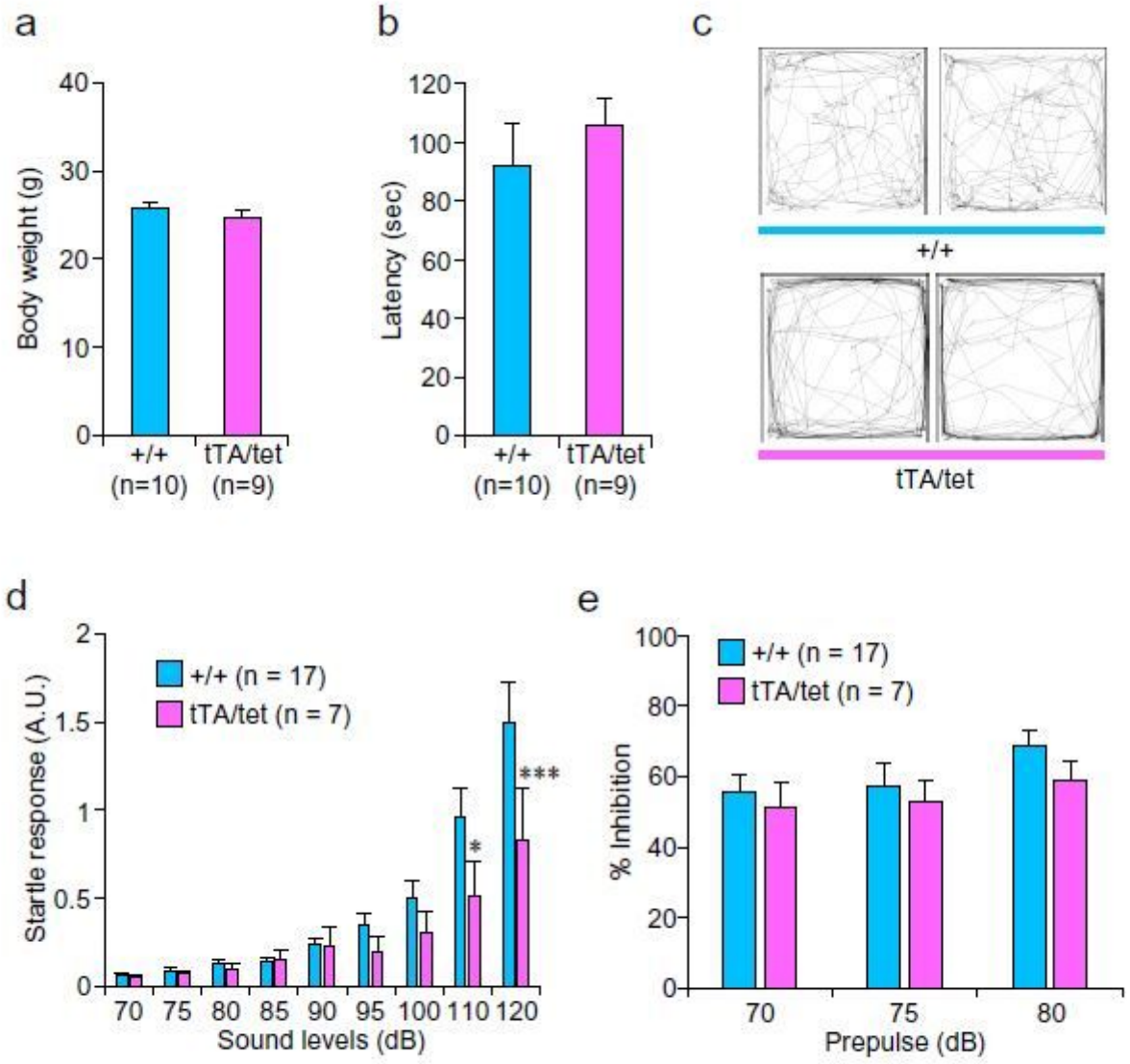

Figure 5

Behavioral consequences of GAD67 knockdown in mice. Body weights (a) and latency to fall from a cylinder in the rotarod test (b) for Dox-treated Gad1+/+ and Gad1tTA/STOP-tetO mice. (c) Examples of the path traveled in the open-field test by two Gad1+/+ and two Gad1tTA/STOP-tetO mice treated with Dox. (d) Acoustic startle responses of Dox-treated Gad1+/+ and Gad1tTA/STOP-tetO mice. Startle amplitudes by the sounds indicate the startle responses (A.U.). *p < 0.05 and ***p < 0.001 between genotypes (simple main effect of two-way ANOVA). (e) PPI responses of Dox-treated Gad1+/+ and Gad1tTA/STOP-tetO mice. PPI was defined as the percent decline in the startle response (% Inhibition).